Microbeam resonant x-ray scattering from bromine-substituted bent-core liquid crystals

Yoichi Takanishi,[1] Youko Ohtsuka,[2] Yumiko Takahashi,[3] and Atsuo Iida[4]
[1]*Department of Physics, Kyoto University, Sakyo, Kyoto 606-8502, Japan*
[2]*Research Center, Tokyo Institute of Technology, O-okayama, Meguro-ku, Tokyo 152-8552, Japan*
[3]*Research Institute of Science and Technology, Nihon University, 7-24-1 Narashinodai, Funabashi 274-8501, Japan*
[4]*Photon Factory, Institute of Material Structure Science, 1-1 Oho, Tsukuba, Ibaraki 305-0801, Japan*
(Received 21 July 2009; published 12 January 2010)

We studied the local layer structure in the B2 phase of bromine-substituted bent-core liquid crystals in the cell geometry using microbeam resonant x-ray scattering. In the homochiral state of B2 phase, the 3/2 order satellite peak was observed only when the incident x-ray energy is at the K absorption edge of bromine. This result clearly indicates that the B2 homochiral domain forms two-layer superlattice in adjacent layers, the same as in the rodlike Sm-C_A phase. The work reports on microbeam resonant x-ray scattering experiment from the local layer of the bent-core liquid crystal in the device geometry. Moreover, we can say that bromine is also useful for the analysis of the superstructure of soft materials using resonant x-ray scattering.

DOI: 10.1103/PhysRevE.81.011701 PACS number(s): 42.70.Df, 61.05.cf

I. INTRODUCTION

Since the discovery of the antiferroelectric phase in rodlike liquid crystal molecules [1], complicate phase transitions and subphases which appears between antiferroelectric and ferroelectric ordered phases were extensively discussed from the various view points. Among them, each phase structure has drawn much attention. The first observed ferrielectric phase was called Sm-$C\gamma^*$, and its structure was proposed that the anticlinic and synclinic interlayer ordering with a ratio of 2:1 are regularly formed [2]. This proposed structure was mainly based on the electro-optical studies, while the conventional x-ray diffraction could not distinguish synclinic structure from anticlinic one because the scalar density profiles along the layer normal of both structures are almost the same. In 1998, however, Mach *et al.* adopted resonant x-ray scattering in order to resolve this problem [3]. This technique treats the x-ray susceptibility as a tensor at the absorption edge energy of a specific element. Thus x-ray scattering reflects the orientation of generally asymmetric local bonding environment of the resonant element depending on the polarization of incident x-rays. As a result, the orientational order with different symmetry can be distinguished by measuring resonant scattering satellite peaks. Their first report became a great breakthrough for determination of various smectic-*C* (Sm-*C*) variants, and the study of the super structures of each subphase has been greatly advanced [4–7]. Details of tensor x-ray structure factor in Sm-*C* variant were formulated by Levelut and Pansu [8]. Moreover, Fernandes *et al.* studied the x-ray resonant scattering of prototype antiferroelectric MHPOBC doped with a chemical probe containing a resonant atom, and succeeded in determining the superstructures of Sm-*C* variants despite of low probe concentration [9].

In order to reveal the electro-optical properties, the thin cell structure of device geometry is usually adopted. Since the uniform layer structure or molecular ordering of the novel liquid crystals in a relatively large area is sometimes difficult to obtain, microbeam analysis is preferable. Resonant x-ray scattering is usually very weak compared to the conventional layer diffraction, while the liquid crystal is easily degraded by the high incident x-ray flux density. In this paper we have successfully applied the microbeam resonant x-ray scattering to the characterization of the novel Br-substituted bent-core liquid crystal B2 phase in the cell structure for the first time. To overcome the experimental difficulty, the optimization of experimental conditions, including the suppression of the background scattering and realization of the stable layer structure, have been pursued. We would also like to emphasize the high potential of microbeam resonant x-ray scattering.

II. EXPERIMENTAL

A sample used is 4-Br-14-O-PIMB [10,11], whose chemical structure and phase sequence are shown in Fig. 1. This compound has a bromine atom substituted at the center phenyl ring. By capillary suction, the compound was inserted into a 16–25-μm -thick sandwich cell whose substrates are 80-μm-thick glass coated with indium tin oxide as an electrode. Rubbed polymer was not coated because the bent-core molecules cannot align uniformly by the rubbing process. By gradual cooling (less than $-0.1\ ^\circ$C/min) from the isotropic phase, uniform circular domains with a diameter of about 100 μm in the B2 phase were obtained. The sample temperature measured was about 129 °C, and the layer spacing at this temperature was determined to be $d=46.8$ Å.

X-ray microbeam experiment was performed at BL-4A of the Photon factory (Tsukuba) [12]. The optical geometry is shown in Fig. 2. The incident beam was monochromatized using a double crystal monochromator and was then focused

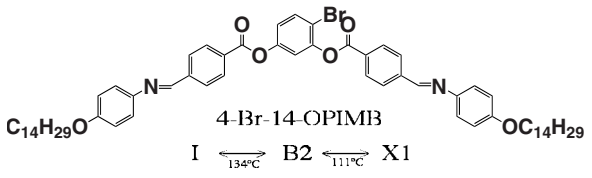

FIG. 1. Chemical structure and phase sequence of the used bent-core liquid crystal with a bromine atom (4-Br-14-O-PIMB).

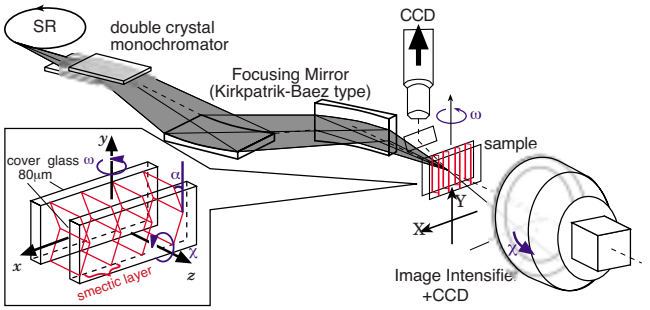

FIG. 2. (Color online) Optical geometry of x-ray microbeam measurement.

using a Kirkpatrick-Baez system down to 3(horizontal) $\times 4$(vertical) μm^2 at the sample. We used a charge coupled device camera (Hamamatsu C4880–50) coupled with an image intensifier as a two dimensional x-ray detector [13]. The sample to camera distance was about 52 cm. To suppress the background intensity the angular divergence of the incident beam was adjusted to the angular spread of the layer diffraction, and the path between the sample and the detector was evacuated to reduce air scattering. In order to avoid the detector saturation due to both the forward scattering and the strong first order smectic layer diffraction, a 2.5-mm-thick aluminum disk plate in addition to a lead direct beam stopper was placed at the center of the detector. The attenuation of x-rays by this disk at the Br absorption edge energy was about 1/1300. To reduce the radiation damage to the sample, the incident photon flux was of the order of 10^7 photons/s. The exposure time for a two-dimensional diffraction pattern was typically ca. 30 min, depending on the signal to background ratio [14].

III. RESULTS AND DISCUSSION

Figure 3 shows the x-ray fluorescence intensity of the Br contained compound as a function of the incident energy (E) around the Br K absorption edge (13.48 keV). The first peak above the absorption edge was used as the resonant energy (E_0).

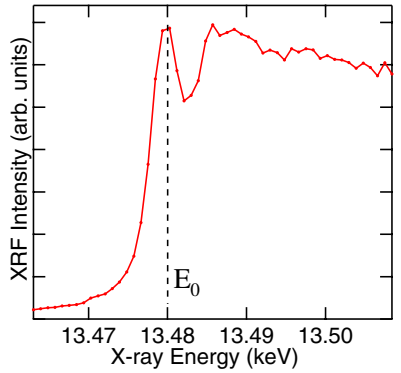

FIG. 3. (Color online) X-ray fluorescence intensity as a function of the incident x-ray energy around the Br K absorption edge from 4-Br-14-O-PIMB. The first peak above the absorption edge was set to resonant edge E_0(=13.48 keV).

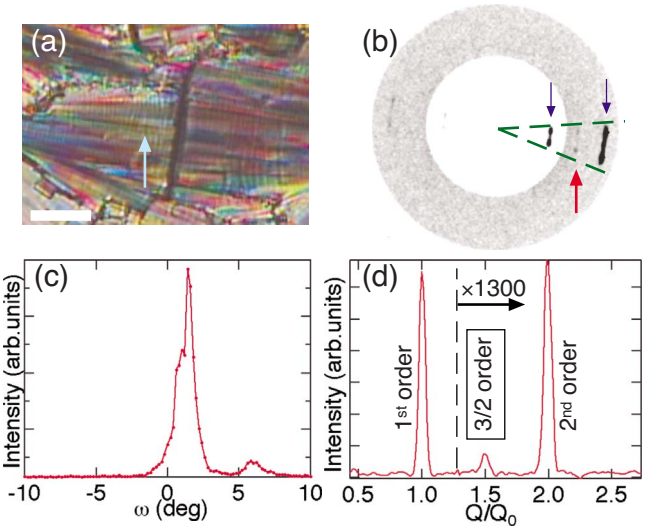

FIG. 4. (Color online) (a) A polarized optical microphotograph of the B2 phase (129.5 °C). An arrow shows the analyzed position. The scale mark shows 100 μm. (b) The two dimensional x-ray scattering profile obtained at the resonant energy. The darker part corresponds to the higher intensity. Thin blue arrows indicate the first and second layer diffraction and a thick red arrow shows the resonant x-ray scattering. The broken lines indicate the angular range to obtain the radial Q scattering intensity profile. (c) The x-ray intensity profile of the first layer diffraction as a function of the ω angle. (d) The radial Q scan profile obtained by integration of 2D x-ray profiles.

Figure 4(a) shows a polarized microphotograph of the irradiated position of B2 domain in which the layer normal is almost parallel to the horizontal direction. For this sample, we applied the high electric field with high frequency enough to induce the transition from Sm-C_AP_A to Sm-C_SP_F [17] for several minutes. After this field treatment, we could obtain the uniform layer structures showing a strong rocking curve peak for the ω and χ scan measurements [see Fig. 4(c)]. Figure 4(b) corresponds to the two dimensional x-ray scattering profile obtained at the incident x-ray energy of E_0. Inner and outer diffraction spots (black arrows) correspond to the first and second layer diffraction, respectively. It is noted that very weak diffraction spots (red arrow) are also observed between two layer peaks, which just corresponds to the 3/2 order diffraction. In order to reveal the layer structure, the x-ray intensity of the first layer diffraction was measured as a function of the ω angle and is shown in Fig. 4(c). The structure was obtained by applying the high electric field for several minutes. From the almost single peak ($\omega=\omega_p$) in this ω-scan and the peak splitting in the χ direction [Fig. 4(b)], the layer structure similar to the horizontal chevron is realized in this small area. In fact, the two-dimensional profile in Fig. 4(b) was obtained at the ω angle for the Bragg condition of the 3/2 order reflection (equal to $\omega_p+0.5\theta_B$). In the resonant condition, the fluorescent intensity is stronger than that in other conditions, and in particular, the background intensity due to the forward scattering increases. Hence the smaller the diffraction angle is, the worse the ratio between peak and background becomes. Therefore, we consider that the 1.5th order peak is easier to obtain than 0.5th

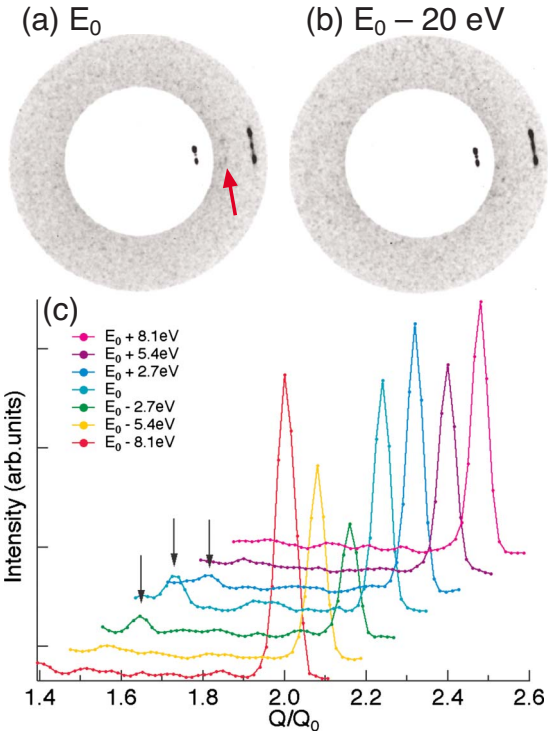

FIG. 5. (Color online) 2D x-ray profile in the homochiral B2 phase when the incident energy is at E_0 (a) and at E_0-20 eV (a). A red arrow indicates the resonant x-ray scattering. (c) A series of radial Q scan profiles as a function of the incident energy around Eo for 3/2- and second order reflections. Arrows indicate 3/2-order reflections.

order peak. Since first- and second-order peaks are quite strong in addition to the sample mosaicity concluded from 1.6 deg. of full width at half maximum of the rocking curve in Fig. 4(b), they are observed even in the incomplete Bragg condition. The two-dimensional intensity distribution was integrated over the appropriate angular range and then the background was subtracted resulting in the radial scattering intensity profile in Fig. 4(d). The strong diffraction peaks at $q=q_0(=2\pi/d=1.34\times10^{-1}$ Å^{-1}) and $2q_0$ correspond to the first- and second-order diffraction peaks, and the weak peak between them just appears at $3/2q_0$, suggesting the two-layer super lattice structure in the B2 phase.

The 3/2 order reflection was appeared when the incident energy is at $E=E_0$, while it disappears at $E=E_0-20$ eV [see Figs. 5(a) and 5(b)]. The detailed incident energy dependence of the 3/2 order resonant peak along with the second-order diffraction are shown in Fig. 5(c). The resonant peak appears only within $E=E_0\pm5.4$ eV. This energy dependence is the strong evidence that the 3/2 order reflection is the resonant x-ray scattering peak and is due to the two layered superlattice.

In order to compare the orientational dependence, the domain in which the layer normal was vertically oriented was also measured [Fig. 6(a)]. The 3/2 order peak spots appeared again as shown in Fig. 6(b) as well as the first- and second-order peaks. Though the incidence angle was not optimized for the Bragg condition of the 3/2 order reflection in this case, the resonant satellite peaks from the domains, where

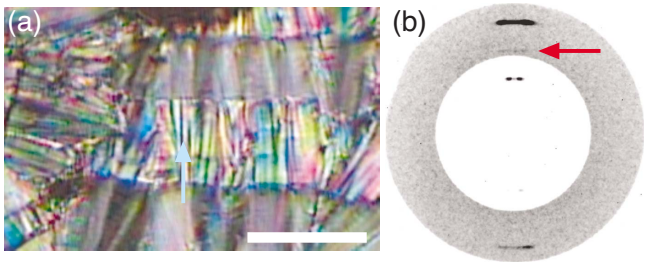

FIG. 6. (Color online) (a) A polarized optical microphotograph of the B2 phase (129.5 °C). An arrow shows the analyzed position. The scale mark shows 100 μm. (b) The two dimensional x-ray scattering profile obtained at the resonant energy. A red arrow indicates the resonant x-ray scattering.

the layer orientation direction is normal to each other, are observed under the horizontally polarized incident x-rays (π- and σ polarized for Figs. 4 and 6, respectively).

These resonant x-ray scattering observations show that the two-layer superlattice structure is realized in these domains. Hence the B2 phase of this compound has anticlinic or antiferroelectric order (Sm-C_AP_A, Sm-C_SP_A or Sm-C_AP_F) [15,16]. Although the polarization analysis of resonant peak is necessary to distinguish them further as reported in Ref. [17], it is difficult to investigate the details at present due to the weak scattered intensity, the lack of the long-time stability of the texture and also to the geometrical constraint of the cell structure. From the difference of the texture under the applied electric field from one without the field, this profile is found to be Sm-C_AP_A.

In addition, we tried to measure the resonant x-ray scattering under the electric field application. Figure 7(a) shows a polarized microphotograph of the irradiated position of the B2 phase during the application of square wave field of ±60 V with 2.1 kHz. The irradiated position is almost the same as Fig. 6(a), and we can see the color change due to the increase in the optical birefringence and the rotation of the dark brushes. These changes clearly indicate the field induced transition from Sm-C_AP_A to the Sm-C_SP_F state. Figure 7(b) shows the two-dimensional x-ray profile obtained from Fig. 7(a) at $E=E_0$. Unlike Fig. 6(b), the 3/2-order satellite peak is not observed, which is consistent with the optical texture indicating the Sm-C_SP_F structure. After turning off the field, the 3/2-order peak appears again, although the in-

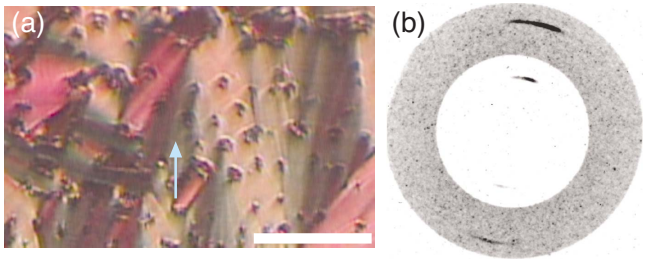

FIG. 7. (Color online) (a) A polarized optical microphotograph of the B2 phase (129.5 °C) under the high field application (square wave of ±60 V at 2.1 kHz). An arrow shows the irradiated position. The scale mark shows 100 μm. (b) The two-dimensional x-ray scattering profile obtained at the resonant energy.

tensity decreases due to the small change of the layer orientation by the high field application for the long time.

So far the target element of the successful resonant x-ray scattering experiment for liquid crystal studies have been almost sulfur [3,4,18], selenium [4,7–9], and chlorine [18]. Sulfur and Chlorine are popular for organic materials, but the K absorption edge energy of them are too low for the conventional x-ray experiment. Se contained antiferroelectric liquid crystals have been successfully analyzed in the device geometry due to the relatively high Se absorption edge energy [4,7].

Bromine is popular as a substituted group of liquid crystal compounds. Though a few reports using the Br-substituted liquid crystals were published [6,9], the resonant x-ray scattering was hardly observed. Cluzeau *et al.* [6] reported that the 3/2-order intensity was extremely low (as strong as 2×10^{-4} compared to the second-order reflection), and considered two reasons in this point as follows: (1) since their used compound has Br atom near the terminal chain, it is hard to reflect the system symmetry (or the molecular anisotropy); (2) the intrinsic scattering ability of Br may be weak. In our case, on the other hand, the intensity of $3/2q_0$ peak was 1/10 as large as that of second-order peak. Hence at least their second reason is not plausible, and our present result strongly suggests that the position of the target atom may be important for the resonant x-ray scattering experiment. Therefore our result demonstrates that Br as well as Se is useful for the analysis of the super structure of soft materials using resonant x-ray scattering technique.

IV. SUMMARY

As a summary, we investigated the local layer structure of the B2 phase using x-ray microbeam resonant scattering. We succeeded in observing the satellite peak reflecting the superlattice using resonant scattering of a pure bromine-substituted bent-core compound, which was said to less effective for the resonant experiment. This work demonstrates the high performance (potential) of x-ray microbeam resonant scattering. We also want to emphasize that bromine atom is effective as a target atom of organic compounds for the resonant x-ray scattering study.

ACKNOWLEDGMENTS

We are thankful to Professor J. Watanabe and Dr. S. Kang for supplying the bent-core compound. This work was carried out under approval of the Photon Factory Advisory Committee (Proposals No. 06G345 and No. 07G592).

[1] A. D. L. Chandani, E. Gorecka, Y. Ouchi, H. Takezoe, and A. Fukuda, Jpn. J. Appl. Phys., Part 2 **28**, L1265 (1989).
[2] H. Takezoe, J. Lee, Y. Ouchi, and A. Fukuda, Mol. Cryst. Liq. Cryst. **202**, 85 (1991).
[3] P. Mach, R. Pindak, A. M. Levelut, P. Barois, H. T. Nguyen, C. C. Huang, and L. Furenlid, Phys. Rev. Lett. **81**, 1015 (1998).
[4] L. S. Hirst, S. J. Watson, H. F. Gleeson, P. Cluzeau, P. Barois, R. Pindak, J. Pitney, A. Cady, P. M. Johnson, C. C. Huang, A. M. Levelut, G. Srajer, J. Pollmann, W. Caliebe, A. Seed, M. R. Herbert, J. W. Goodby, and M. Hird, Phys. Rev. E **65**, 041705 (2002).
[5] L. S. Matkin, S. J. Watson, H. F. Gleeson, R. Pindak, J. Pitney, P. M. Johnson, C. C. Huang, P. Barois, A. M. Levelut, G. Srajer, J. Pollmann, J. W. Goodby, and M. Hird, Phys. Rev. E **64**, 021705 (2001).
[6] P. Cluzeau, P. Gisse, V. Ravaine, A.-M. Levelut, P. Barois, C. C. Huang, F. Rieutord, and H. T. Nguyen, Ferroelectrics **244**, 1 (2000).
[7] P. D. Brimicombe, N. W. Roberts, S. Jaradat, C. Southern, S.-T. Wang, C.-C. Huang, E. DiMasi, R. Pindak, and H. F. Gleeson, Eur. Phys. J. E **23**, 281 (2007).
[8] A. M. Levelut and B. Pansu, Phys. Rev. E **60**, 6803 (1999).
[9] P. Fernandes, P. Barois, E. Grelet, F. Nallet, J. W. Goodby, M. Hird, and J.-S. Micha, Eur. Phys. J. E **20**, 81 (2006).
[10] S. Edo, X. Li, M. Tokita, S. Kang, and J. Watanabe, Jpn. J. Appl. Phys. **48**, 030215 (2009).
[11] S. Kang, M. Tokita, K. Ogino, T. Doi, T. Takahashi, H. Takezoe, and J. Watanabe, Phys. Rev. E **73**, 011701 (2006).
[12] A. Iida, K. Noma, and K. Hirano, Ferroelectrics **149**, 117 (1993).
[13] Y. Takanishi, H. Takezoe, J. Watanabe, Y. Takahashi, and A. Iida, J. Mater. Chem. **16**, 816 (2006).
[14] Y. Takanishi, M. Toshimitsu, M. Nakata, N. Takada, T. Izumi, K. Ishikawa, H. Takezoe, J. Watanabe, Y. Takahashi, and A. Iida, Phys. Rev. E **74**, 051703 (2006).
[15] D. R. Link, G. Natale, R. Shao, J. E. Maclennan, N. A. Clark, E. Korblova, and D. M. Walba, Science **278**, 1924 (1997).
[16] H. Takezoe and Y. Takanishi, Jpn. J. Appl. Phys., Part 1 **45**, 597 (2006).
[17] P. Fernandes, P. Barois, S. T. Wang, Z. Q. Liu, B. McCoy, C. C. Huang, R. Pindak, W. Caliebe, and H. T. Nguyen, Phys. Rev. Lett. **99**, 227801 (2007).
[18] A. Cady, R. Pindak, W. Caliebe, P. Barois, W. Weissflog, H. T. Nguyen, and C. C. Huang, Liq. Cryst. **29**, 1101 (2002).